Engineering Structures 196 (2019) 109313

Contents lists available at ScienceDirect

Engineering Structures

journal homepage: www.elsevier.com/locate/engstruct

Time-varying system identification by enhanced Empirical Wavelet Transform based on Synchroextracting Transform

Yu Xin[a], Hong Hao[a], Jun Li[a,b,*]

[a] Centre for Infrastructural Monitoring and Protection, School of Civil and Mechanical Engineering, Curtin University, Kent Street, Bentley WA6102, Australia
[b] School of Civil Engineering, Guangzhou University, Guangzhou 510006, China

ARTICLE INFO

Keywords:
Time-varying system
Empirical Wavelet Transform
Synchroextracting Transform
Instantaneous frequency
Bridge-vehicle system

ABSTRACT

In this paper, an enhanced Empirical Wavelet Transform (EWT) approach based on Synchroextracting Transform (SET) is proposed for time-varying system identification. When a structure of time-varying physical properties, i.e. mass, stiffness or damping, is under external excitations, structural dynamic responses are usually non-stationary because the system has time-varying dynamic vibration characteristics. Under this circumstance, it would be difficult to determine the number of Intrinsic Mode Functions (IMFs) included in structural dynamic responses by using Fourier spectrum. Considering that the filtering boundaries of traditional EWT method are defined based on the segmental Fourier Spectrum of a processed signal, directly using it for non-stationary signal decomposition may not be effective and accurate. To apply the EWT method for time-varying system identification, in this study, time-frequency analysis based on SET is first performed to determine the frequency components of a non-stationary vibration signal instead of using Fourier spectrum. The filtering boundaries for EWT analysis are determined based on the time-frequency representation. Then, the IMFs are extracted from the non-stationary vibration signals by using EWT with the above defined filtering boundaries. When the IMFs are accurately obtained, the instantaneous frequencies of IMFs are identified by using Hilbert Transform (HT). In numerical simulations, a simulated signal with a high level noise is analyzed to verify the feasibility of using SET to define the filtering boundaries. Then the proposed approach is used to identify the instantaneous frequencies of a time-varying two-storey shear type building under earthquake and Gaussian white noise excitations, respectively. Experimental investigations on a time-varying bridge-vehicle system are conducted to verify the effectiveness of the proposed approach. The results in both numerical simulations and experimental validations demonstrate that the enhanced EWT approach can effectively and reliably identify the instantaneous frequencies of time-varying systems.

1. Introduction

Dynamic behaviors of engineering structures often change over time due to the environmental condition changes, mass and stiffness changes due to the material loss or strength degradation, and the effects of extreme loads, etc. These time-varying system effects can be widely observed in many engineering fields, i.e. civil and mechanical engineering. For example, the friction mechanisms used in industry can introduce the changes in the stiffness and damping of a structure under normal operations. Civil structures may also exhibit time varying vibration characteristics under earthquake, tornados and hurricanes, because of the nonlinearities in the structures, and the changes in the stiffness and boundary conditions [1]. Therefore, identifying the vibration characteristics of time-variant structures is vital for researchers and engineers to understand and assess the operational conditions of structures.

Over the past decades, system identification of time-variant structures based on the measured vibration responses (i.e. acceleration, displacement responses) has obtained a broad attention. Various techniques have been developed and reported in the literatures [2,3]. Generally, these methods could be classified into two categories: (1) time-varying system identification based on adaptive algorithms [4–6]; (2) Time-varying system identification by using time-frequency analysis techniques [7–9]. For example, Wang et al. [3] used a least-squares (LS) parameter estimation method with slide-window function to track the real-time frequency of a high-voltage switch structure under the cyclic loading excitations in the laboratory. Yang et al. [6] proposed a novel LS parameter estimation approach to adaptively track the system

* Corresponding author at: Centre for Infrastructural Monitoring and Protection, School of Civil and Mechanical Engineering, Curtin University, Kent Street, Bentley WA6102, Australia.
E-mail addresses: yu.xin@postgrad.curtin.edu.au (Y. Xin), hong.hao@curtin.edu.au (H. Hao), junli@curtin.edu.au, LI.Jun@connect.polyu.hk (J. Li).

https://doi.org/10.1016/j.engstruct.2019.109313
Received 27 March 2019; Received in revised form 16 June 2019; Accepted 17 June 2019
Available online 21 June 2019
0141-0296/

parameters of a time-variant structure. In addition, in the literature [10], an improved LS strategy is developed to identify the hysteretic parameters of a nonlinear system under arbitrary external excitations.

In recent years, time-frequency analysis techniques have been widely conducted for system identification of time-variant structures, i.e. by using Hilbert Transform (HT) [11,12] and Wavelet Transform (WT) [13–15]. Shi et al. [16] applied Empirical Mode Decomposition (EMD) with HT for the modal parameter identification of a time-varying multi-degree-of-freedom (MDOF) system. Bao et al. [2] developed an improved Hilbert-Huang Transform (HHT) method for time-varying system identification by using the autocorrelation functions of structural dynamic responses as the input to HHT, and therefore reduced the noise effect and improved the accuracy of identification. Wang et al. [17] proposed a recursive HT system identification approach, which have been successfully used to track the real-time structural characteristics of linear shear-type buildings under the forced vibration. WT is an alternative time-frequency analysis approach, which has been widely used for the system identification of linear and non-linear structures. Hou et al. [18] developed a novel approach for instantaneous modal identification of a time-varying structure subjected to an earthquake excitation based on continuous wavelet transform (CWT). Wang et al. [7] used the extracted wavelet ridges to effectively identify the instantaneous frequency (IF) of a cable structure with different tension forces under the stochastic excitations.

More recently, a new time-frequency analysis technique, named Synchrosqueezing Transform (SST), has been developed by Daubechies et al. [19], and has been applied for IF identification [20,21]. The main advantage of SST is that it squeezes the time-frequency coefficients into the IF trajectory, which can be approximated to an ideal tine-frequency analysis representation. However, SST has a lower time-frequency resolution when it is used to reconstruct the interested components of a non-stationary signal. Based on the theory of SST, a novel time-frequency analysis method, namely Synchroextracting Transform (SET), have been developed by Yu et al. [22], which can generate a more energy-concentrated analysis result than using SST.

In this study, time-frequency representation based on SET is employed to detect the filtering boundaries of the Empirical Wavelet Transform (EWT) process [23] for non-stationary signal analysis. In the past studies, several modified EWT methods have been successfully applied for operational modal identification [24,25]. However, to the authors' best knowledge, there has been no study yet on using or improving EWT method for IF identification of time-varying structures. With the vibration responses measured from a time-varying structure, time-frequency analysis based on SET is first performed to determine the filtering boundaries of EWT instead of using the ordinary Fourier Spectrum. Then EWT is applied to extract the individual modes from the vibration response signals. Each mode is an amplitude-modulation and frequency-modulation signal with a narrow-band property with a varying IF. The IF of each time-variant component can be identified by using HT. A synthetic signal which consists of two time-varying frequency components is first used to verify the feasibility and accuracy of the proposed approach. Then the proposed method is employed to identify the IF of a two-storey shear-type building under the forced vibration. Experimental studies on a real bridge under the heavy traffic loads are conducted to further validate the effectiveness of the proposed method.

The remainder of this paper is organized as follows. Section 2 briefly explains the principle of EWT and SET, and provides a fundamental process of time-varying system identification based on the proposed approach. In Section 3, numerical studies on a synthetic signal and a two-storey time-varying structure are conducted to investigate the accuracy and effectiveness of the proposed approach. In Section 4, Experimental verifications on a highway bridge under the traffic loads are performed to identify the instantaneous frequencies. Section 5 provides the discussions and conclusions on the obtained results.

2. Theoretical background and development

2.1. Empirical Wavelet Transform (EWT)

Using the traditional EWT method for vibration signal decomposition consists of two main steps: (1) Segmenting the Fourier spectrum of the target vibration signal; (2) Constructing the filtering bank, and processing each segmental part of the signal. To determine the filtering banks of the EWT method, the local peaks of the Fourier spectrum are firstly identified. The lowest local minima between the two sequential peaks are detected, which are defined as the boundaries of each filtering bank.

Assuming that the Fourier spectrum of a vibration signal is divided into N segments, the boundaries of all segments can be denoted as $\omega_n (n = 0, 1, \cdots, N)$, and the filtering boundaries of each segment can be defined by an interval $\Omega_n = [\omega_{n-1}, \omega_n]$ (where $\omega_0 = 0 \text{and} \omega_N = \pi$). It is noted that $\bigcup_{n=1}^{N} \Omega_n = [0, \pi]$. A transient phase with a width of $2\tau_n$ is defined for each ω_n, and τ_n can be written as

$$\tau_n = \gamma \times \omega_n \tag{1}$$

$$0 < \gamma < min_n \frac{\omega_{n+1} - \omega_n}{\omega_{n+1} + \omega_n} \tag{2}$$

In the literature [23], the basic function used for the EWT analysis is Meyer wavelet, and the corresponding scaling function and the empirical wavelets are expressed as

$$\widehat{\varnothing}_n(\omega) = \begin{cases} 1 & \text{if } |\omega| \le (1-\gamma)\omega_n \\ \cos\left[\frac{\pi}{2}\beta\left(\frac{1}{2\gamma\omega_n}(|\omega| - (1-\gamma)\omega_n)\right)\right] & \text{if}(1-\gamma)\omega_n \le |\omega| \le (1+\gamma)\omega_n \\ 0 & \text{oherwise} \end{cases} \tag{3}$$

$$\widehat{\Psi}_n(\omega) = \begin{cases} 1 & \text{if}(1+\gamma)\omega_n \le |\omega| \le (1-\gamma)\omega_{n+1} \\ \cos\left[\frac{\pi}{2}\beta\left(\frac{1}{2\gamma\omega_{n+1}}(|\omega| - (1-\gamma)\omega_{n+1})\right)\right] & \text{if}(1-\gamma)\omega_{n+1} \le |\omega| \le (1+\gamma)\omega_{n+1} \\ \sin\left[\frac{\pi}{2}\beta\left(\frac{1}{2\gamma\omega_n}(|\omega| - (1-\gamma)\omega_n)\right)\right] & \text{if}(1-\gamma)\omega_n \le |\omega| \le (1+\gamma)\omega_n \\ 0 & \text{oherwise} \end{cases} \tag{4}$$

where $\beta(x)$ denotes the auxiliary function of the Meyer wavelet, which can be defined as [23]

$$\beta(x) = \begin{cases} x^4(35 - 84x + 70x^2 - 20x^3) & \forall\, x \in (0, 1) \\ 0 & x \le 0 \\ 1 & x \ge 1 \end{cases} \tag{5}$$

When the scaling function and empirical wavelets mentioned in Eqs. (3) and (4) are derived, the EWT analysis is conducted and the detail coefficients can be expressed as

$$W_x(n, t) = \int x(\tau)\Psi_n(\tau - t)d\tau = F^{-1}(\widehat{X}(\omega)\overline{\widehat{\Psi}_n(\omega)}) \tag{6}$$

The approximation coefficients can be obtained by

$$W_x(0, t) = \int x(\tau)\varnothing_n(\tau - t)d\tau = F^{-1}(\widehat{X}(\omega)\overline{\widehat{\varnothing}_n(\omega)}) \tag{7}$$

Then, the modes extracted from the vibration signal are described as

$$f_0(t) = W_x(0, t) * \varnothing_1(t) \tag{8}$$

$$f_k(t) = W_x(k, t) * \Psi_k(t) \tag{9}$$

and the reconstruction signal can be obtained as

$$\begin{aligned} \hat{x}(t) &= W_x(0, t) * \varnothing_1(t) + \sum_{n=1}^{N} W_x(n, t) * \Psi_n(t) \\ &= F^{-1}\left(W_x(0, \omega)\widehat{\varnothing}_1(\omega) + \sum_{n=1}^{N} \widehat{W}_x(n, \omega) * \widehat{\Psi}_n(\omega)\right) \end{aligned} \tag{10}$$

2.2. The improved EWT approach

As mentioned in a previous study [24], it is a significant challenge

to use the traditional Fourier Spectrum for determining the filtering boundaries associated with EWT analysis when a signal is contaminated by significant noise and non-stationary components. Therefore, an improved time-frequency analysis approach is worth of investigations to identify and track the real-time frequency components of the non-stationary signals. With an improved energy-concentration of the time-frequency representation, in this study, SET is employed to enhance the process for filtering boundary detection when the EWT method is conducted for non-stationary signal decomposition.

2.2.1. Synchroextracting Transform (SET)

A multicomponent vibration signal$x(t)$, which consists of N non-stationary frequency components, is presented as

$$x(t) = \sum_{i=1}^{N} x_i(t) = \sum_{i=1}^{N} A_i(t) e^{j\int \omega_i(t)dt} \tag{11}$$

in which $A_i(t)$ and $\omega_i(t)$ represent the amplitude and frequency information of the ith time-varying component, respectively. The different modes can be well separated based on a sufficient distance, i.e.,

$$\omega_{i+1}(t) - \omega_i(t) > 2\Delta, j \in \{1, \cdots, m-1\} \tag{12}$$

where Δ denotes the frequency support of the window function. The Short Time Fourier Transform (STFT) representation $G_e(t, \omega)$ of the vibration signal $x(t)$ can be derived by using the first-order approximation form [22,26,27]

$$G_e(t, \omega) \approx \sum_{i=1}^{N} A_i(t) * \hat{g}(\omega - \omega_i(t)) e^{j\int \omega_i(t)dt} \tag{13}$$

in which $\hat{g}(\cdots)$ denotes the Fast Fourier transform.

Then, the IF of the vibration signal is derived using

$$\omega(t) = \sum_{i=1}^{N} \omega_i(t) = -j * \frac{\partial G_e(t, \omega)}{G_e(t, \omega)} \tag{14}$$

To generate an energy-concentrated time-frequency representation, the Fourier-based SST is proposed by Oberlin et al. [27], which can be expressed as

$$Ts(t, \omega) = G_e(t, \omega) * \delta_1(\omega - \omega_i(t)) \tag{15}$$

When SST is performed based on the original STFT coefficients of a multi-component vibration signal, the discrete coefficients will be squeezed into the IF trajectory$\omega_i(t)$ from the original results of$G_e(t, \omega)$. Based on the post-processing procedure of SST, a sharper energy-concentrated time-frequency representation can be realized than the original STFT results [27]. However, when the target signals are contaminated with measurement noise, the noise will also affect the time-frequency analysis results by SST, which may lead to a poor noise robustness. To overcome this problem, Yu et al. [22] proposed to retain only the time-frequency information of the STFT results which are significantly related to the time-variant characteristics of a vibration signal. In this case, SET is expressed as

$$Te(t, \omega) = G_e(t, \omega) * \delta_2(\omega - \omega_i(t)) \tag{16}$$

where $\delta_2(\omega - \omega_i(t))$ can be further expressed as

$$\delta_2(\omega - \omega_i(t)) = \begin{cases} 1, & \omega = \omega_i(t) \\ 0, & else \end{cases} \tag{17}$$

Based on Eq. (17), it can be observed that the term $\delta_2(\omega - \omega_i(t))$ extracts the time-frequency coefficients of $G_e(t, \omega)$ in the IF trajectories, and the residual coefficients are removed. By using SET method, a more energy-concentrated representation can be obtained than using SST. Therefore the time-frequency resolution is highly enhanced. In addition, since using SET only retains the STFT coefficients which have the maximum values, the effect of measurement noise can be significantly decreased.

2.2.2. Time-varying system identification based on the improved EWT

For an n degree-of-freedom (DOF) time-variant system, the equation of motion is given as

$$\mathbf{M}(t)\ddot{\boldsymbol{u}}(t) + \mathbf{C}(t)\dot{\boldsymbol{u}}(t) + \mathbf{K}(t)\boldsymbol{u}(t) = \mathbf{f}(t) \tag{18}$$

in which$\mathbf{M}(t)$, $\mathbf{K}(t)$, and $\mathbf{C}(t)$ denote the time-variant mass, stiffness and damping matrices, respectively; $\boldsymbol{u}$(t), $\dot{\boldsymbol{u}}$(t)and$\ddot{\boldsymbol{u}}$(t) are displacement, velocity and acceleration response vectors of the time-variant system; $\mathbf{f}(t)$ is the external excitation force vector.

For Eq. (18), it can be further transformed into modal spatial coordinates [1], which can be expressed as

$$\ddot{q}_i(t) + 2h_{0i}\dot{q}_i(t) + \omega^2{}_{0i}q_i(t) = \frac{\varnothing_i^T \mathbf{f}(t)}{\boldsymbol{M_i}} \qquad (i = 1, 2, \cdots n) \tag{19}$$

where $\boldsymbol{M_i} = \varnothing_i^T \mathbf{M} \varnothing_i$ denotes the ith modal mass, $\varnothing_i$ is the ith mode shape vector. The natural frequency of the ith modal response is represented byω_{0i}. When zero-mean Gaussian white noise is assumed as the input of the system, the IF of the ith modal response can be written as

$$\omega^2{}_i(t) = \omega^2{}_{0i}(t) - \frac{\frac{\varnothing_i^T \mathbf{f}(t)}{\boldsymbol{M_i}} q + H\left[\frac{\varnothing_i^T \mathbf{f}(t)}{\boldsymbol{M_i}}\right] H[q]}{[q^2 + (H[q])^2]} \tag{20}$$

where $H[\ ]$ denotes HT, and the second term in Eq. (20) is about a fast time-varying function with the mean value equals to zero. The instantaneous natural frequencies of the time-varying system during the vibration are extracted from the identified frequencies by filtering out the fast varying component.

The measured dynamic response of the l-th DOF $u_l(t)$ of the time-varying system can be described as a function of modal responses

$$u_l(t) = \sum\nolimits_{i=1}^{n} \phi_{li} q_i \tag{21}$$

where ϕ_{li} is the l-th coefficient of the i-th mode shape vector. The decomposed ith modal response$u_l{}^{(i)}(t)$ of the measured vibration signal from the l-th DOF can be represented as

$$u_l{}^{(i)}(t) = \phi_{li} q_i \tag{22}$$

The obtained mono-component signal$u_l{}^{(i)}(t)$can be written as an analytical signal$Z_l{}^{(i)}(t)$

$$Z_l{}^{(i)}(t) = \phi_{li} q_i + \phi_{li} H[q_i] = \phi_{li} A_i e^{j\int \omega_i(t)dt} \tag{23}$$

From Eq. (23), it suggests that the identified IF of the i-th decomposed dynamic response equals to the IF of the i-th modal response. In this study, an improved EWT process with HT is applied for time-variant system identification, and the proposed strategy is shown in Fig. 1.

3. Numerical studies

3.1. A simulation signal

In this section, a simulated signal$y(t)$, as defined in Eq. (24), is used to investigate the effectiveness of using SET to determine the boundaries for EWT analysis. It consists of two time-variant frequency components$y_1(t)$ and$y_2(t)$ which are described in Eqs. (25) and (26), respectively.

$$y(t) = y_1(t) + y_2(t) + noise(t) \tag{24}$$

$$y_1(t) = 2\sin(14\pi t + 4\pi \arctan((2t-2)^2)) \tag{25}$$

$$y_2(t) = 2\sin(48\pi t + 20\pi \sin t) \tag{26}$$

To further validate the feasibility of using SET to improve the performance of EWT, a high-level noise, that is, 20% Gaussian white noise, is added to the simulated signal. The sampling duration is set as 5 s with a sampling rate of 120 Hz. Figs. 2 and 3 show the vibration signal and the corresponding Fourier Spectrum, respectively. It can be observed

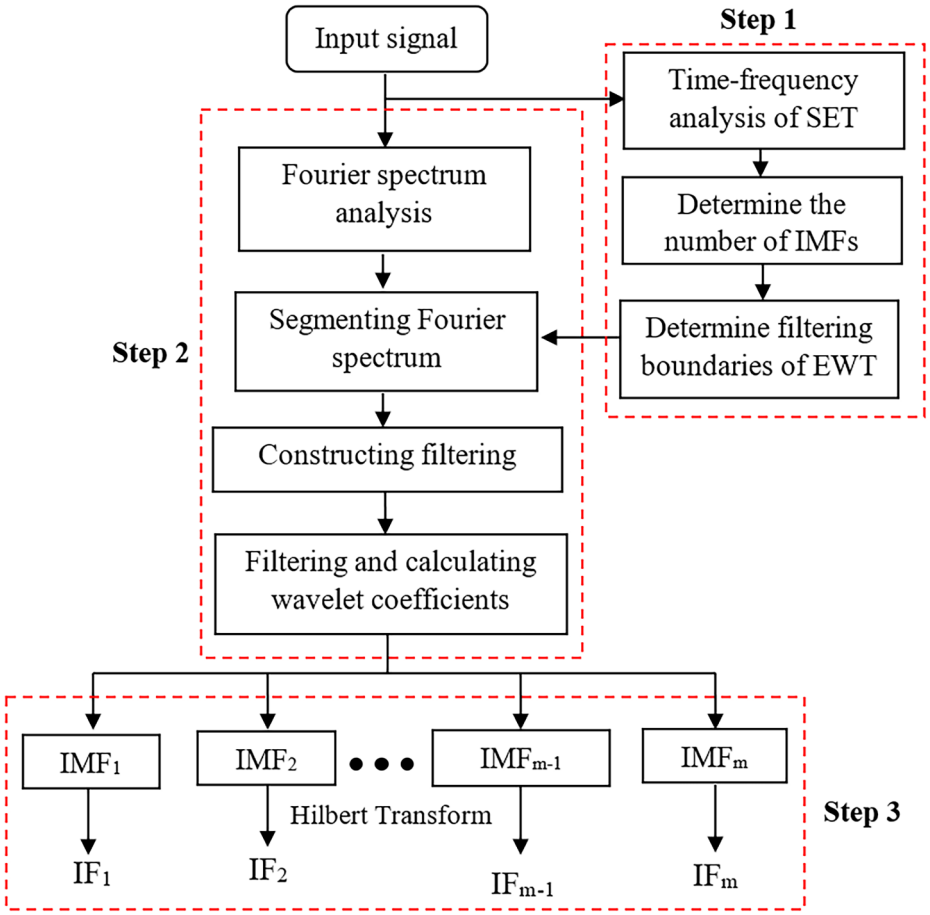

Fig. 1. The flowchart of time-variant system identification using the improved EWT.

from Fig. 3 that the two frequency components are not obvious and therefore properly defining the filtering boundaries for EWT analysis may not be straightforward. Under this circumstance, the time-frequency analysis based on the SET is used to track and determine the varying frequency components of the target signal. To verify the effectiveness of using SET, the classical time-frequency analysis technique, namely WT, is also performed to identify the instantaneous frequencies of the signal. The time-frequency analysis results obtained from WT and SET are described in Fig. 4(a) and (b), respectively. From Fig. 4, it can be observed that the non-stationary signal consists of two time-varying components. To decompose these two mono-components from the target signal by using EWT, a constant filtering boundary should be determined between these two components. By comparing the results in Fig. 4(a) and (b), it can be observed that with a more energy-concentrated time-frequency representation realized by using SET, it is distinguishable to determine the clear constant filtering bounds between two mono-components. In Fig. 4(a), the frequency of the dashed line is calculated based on the maximum frequency of the first frequency component and the lowest value of the second frequency

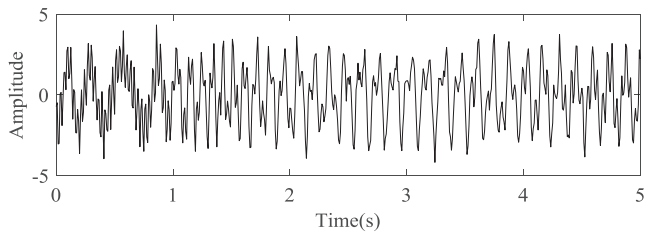

Fig. 2. The simulated signal with 20% noise.

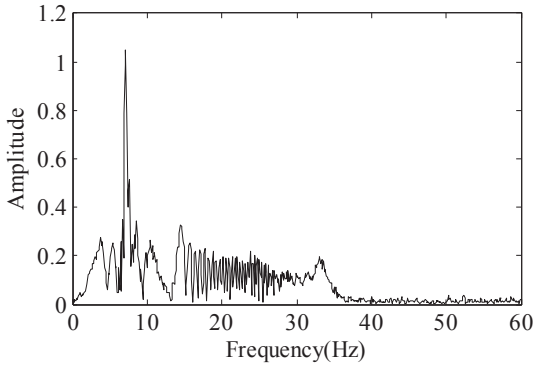

Fig. 3. Fourier Spectrum of the simulated signal.

component. This dash line is used to show that the filtering boundary may not be well selected, due to the insufficient time-frequency analysis resolution by using WT. In real signal decomposition, the constant filtering boundary is usually determined by using

$$\omega_c = \frac{[\omega_1(t)]^{max} + [\omega_2(t)]^{min}}{2} \tag{27}$$

in which $[\omega_1(t)]^{max}$ is the maximum frequency value of the first mono-component, and $[\omega_2(t)]^{min}$ represents the minimum frequency value of the second component.

For WT analysis, the wavelet ridges of two time-varying components are usually firstly identified, and then the filtering boundary can be determined accordingly. Based on Eq. (27), the location of the selected constant filtering boundary by using SET is accurately shown in

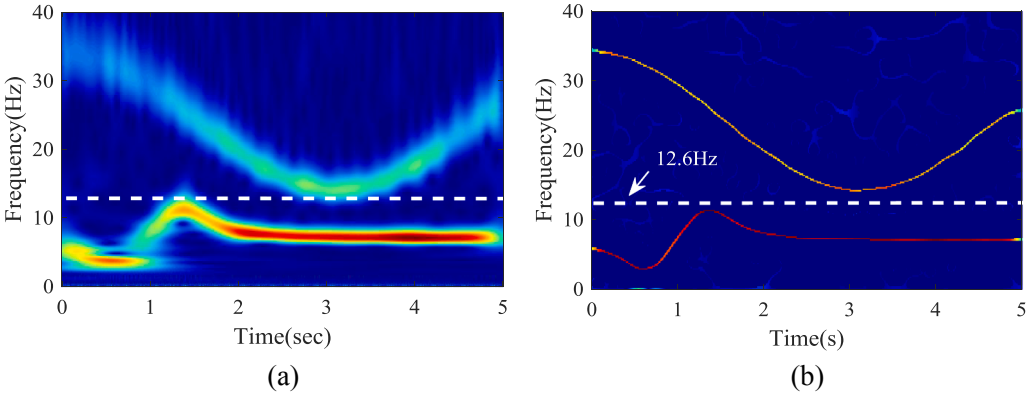

Fig. 4. Time-frequency representation of the simulated signal using: (a) WT; (b) SET.

Fig. 4(b). Once the filtering boundaries are exactly determined, the Fourier Spectrum of the non-stationary signal can be segmented for EWT, and used to construct the filtering bank. Then, the individual modes can be effectively decomposed, and the obtained two time-varying IMFs are shown in Figs. 5(a) and 6(a), respectively. To further verify the effectiveness of the proposed approach, Variational Mode Decomposition (VMD) [28] is also performed to identify the time-varying components of the signal, and the decomposed two IMFs are shown in Figs. 5(b) and 6(b), respectively. By comparing the identified results in Figs. 5 and 6, it is clearly observed that the improved EWT is more reliable and accurate to identify the time-varying components of the signal. In addition, Fig. 7(a) and (b) display the Fourier spectrum of the extracted IMFs using two methods, respectively, it can be observed that the non-stationary simulated signal can be accurately decomposed by using the improved EWT approach, even under a significant noise effect.

3.2. A two-storey time-varying shear building

In the section, a two-storey shear building model with the varying structural stiffness, as displayed in Fig. 8, is constructed to validate the feasibility of using the improved EWT process for time-varying system identification. The time-varying structure has two masses of $m_1 = 2.50 \times 10^5$ kg at the first floor, and $m_2 = 1.70 \times 10^5$ kg at the top floor. Two damping coefficients $c_1 = 9.6 \times 10^2$ kN s/m and $c_2 = 3.2 \times 10^2$ kN s/m are assumed for these two stories. To simulate

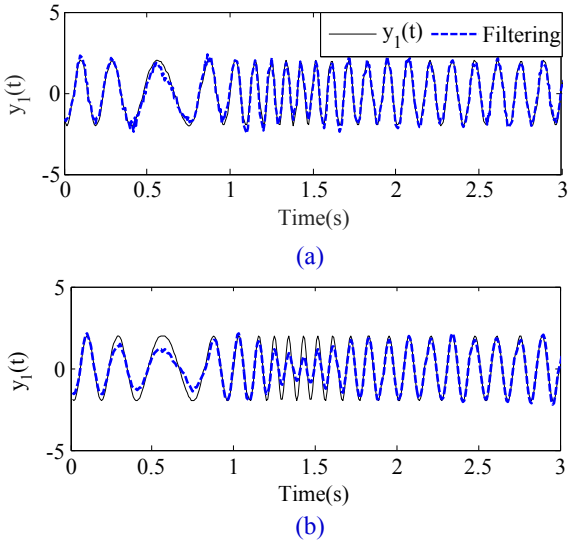

Fig. 5. The decomposed first mono-component using: (a) Improved EWT; (b) VMD.

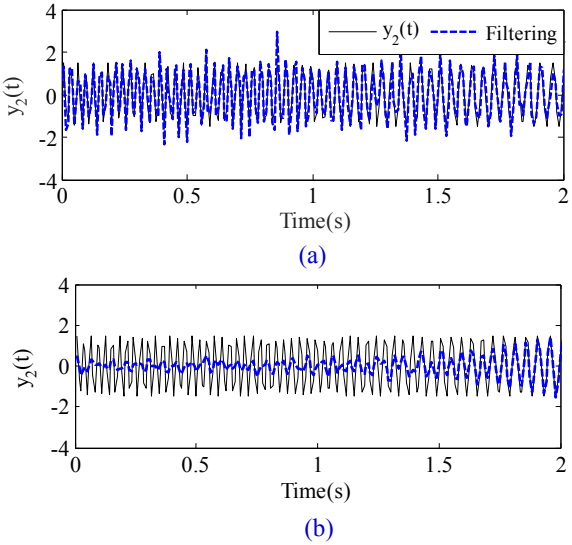

Fig. 6. The decomposed second mono-component using: (a) Improved EWT; (b) VMD.

the time-variant dynamic characteristics of the structure model, two time-variant stiffness coefficients k_1 and k_2 are employed to define the lateral stiffness of the building model. The stiffness coefficients of k_1 is set to be periodically reduced from 2.10×10^5 kN·m to 1.404×10^5 kN·min a time duration between 4 and 16 s, that is, $k_1 = \{2.1 - 0.058(t-4) - 0.131\sin[0.5\pi(t-4)]\} \times 10^5$ kN m. The initial stiffness coefficient ofk_2 is set as 1.05×10^5 kN m, and then, linearly degraded from 1.05×10^5 kN·m to 0.7×10^5 kN·mbetween 4 s and 8 s.

3.2.1. Instantaneous frequency identification

In order to investigate the accuracy and reliability of the improved EWT approach for time-varying system identification, the following two excitations are considered in the numerical case studies.

Case 1: The 1940 El Centro ground acceleration record is employed as the input of the structure, which is shown in Fig. 9(a);
Case 2: A Gaussian white noise series with a standard deviation of 0.1 g (g equals to 9.81 m/s^2) is selected as the external excitation of the structure, as displayed in Fig. 9(b).

For the above mentioned two cases, the structural dynamic responses of the first floor are recorded with a sampling rate of 50 Hz. The recorded displacement responses for the two cases are shown in Fig. 10(a) and (b). Since the non-stationary characteristics of the structural dynamic responses are unknown in prior, SET is first

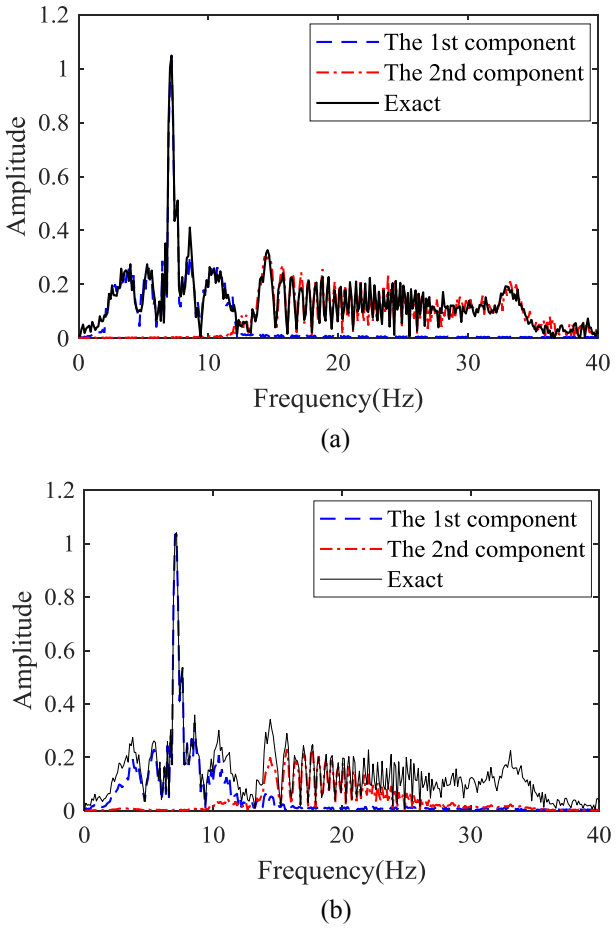

Fig. 7. Fourier spectrum of the two decomposed IMFs using: (a) Improved EWT; (b) VMD.

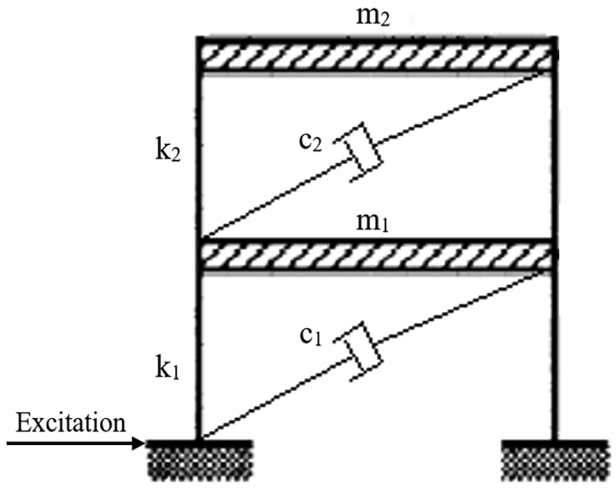

Fig. 8. The two-storey shear building model.

performed to determine the filtering boundaries for EWT analysis. The SET results of these two cases are depicted in Fig. 11 (a) and (b), respectively. As can be seen from Fig. 11, the time-frequency analysis results based on SET method are obviously more fluctuant than those in Section 3.1. The phenomenon is significantly caused from the rapidly varying frequency component contained in structural dynamic responses when the building structure is forced by zero-mean earthquake and Gaussian white noise excitations. However, it can be clearly observed from Fig. 11 that the fluctuations of the two varying frequency

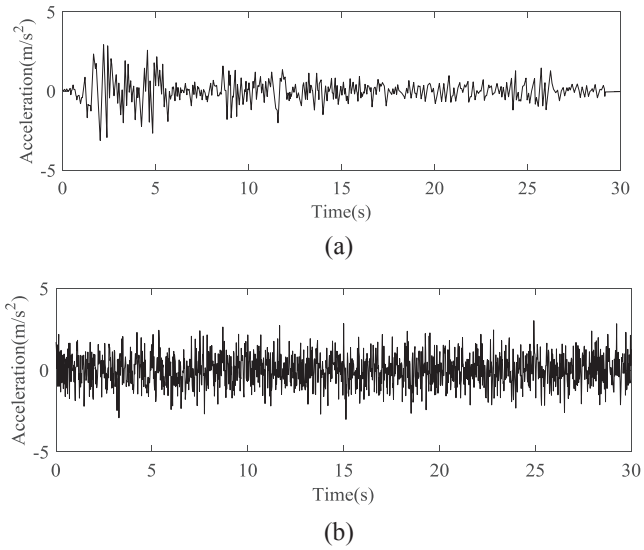

Fig. 9. External excitations in two numerical cases: (a) El Centro earthquake; (b) Gaussian white noise.

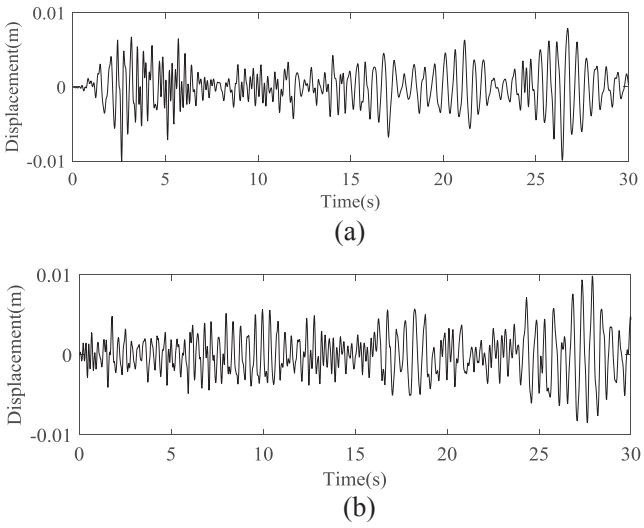

Fig. 10. Displacement responses of the first floor: (a) under earthquake excitation; (b) under Gaussian white noise excitation.

components are respectively located in two separated frequency ranges, which are from 1.4 Hz to 3.0 Hz and 4.5 Hz to 6.8 Hz, respectively. It is noted that SET is mainly used to define the filtering boundaries, and the results clearly indicate that the time-frequency representation based on SET is more reliable for defining the filtering boundaries of EWT analysis. In addition, to verify the effectiveness and improvement of the time-frequency representation based on SET, the analysis result shown in Fig. 11(a) is further compared with those from the other three advanced time-frequency analysis tools, i.e. S-Transform, Wavelet transform and SST methods. The results are shown in Fig. 12. It is observed that the time-frequency representation based on SET is more reliable for defining the filtering boundary with a higher resolution. Therefore, based on the time-frequency representations shown in Fig. 11(a) and (b), the filtering boundaries for the analysis of EWT can be well defined as three constant frequencies, i.e., 0.8 Hz, 3.5 Hz and 7.5 Hz, respectively. Once the filtering boundaries are defined, the two time-varying frequency components of structural displacement responses can be exactly separated by the EWT approach. The identified instantaneous frequencies of the two cases by using HT are presented in Fig. 13(a) and (b). Significant fluctuations are observed by comparing the results from

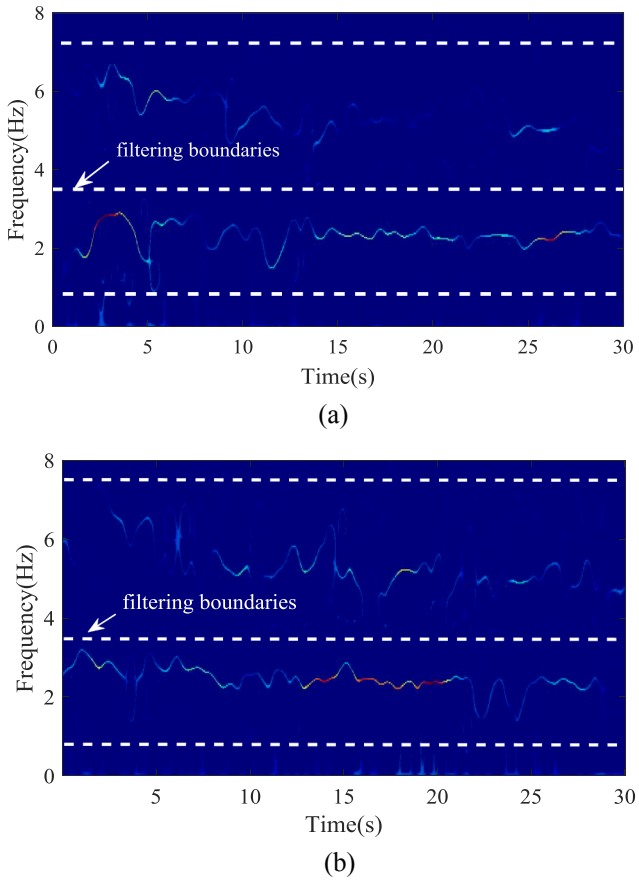

Fig. 11. The detected filtering boundaries based on SET: (a) under earthquake excitation; (b) under Gaussian white noise excitation.

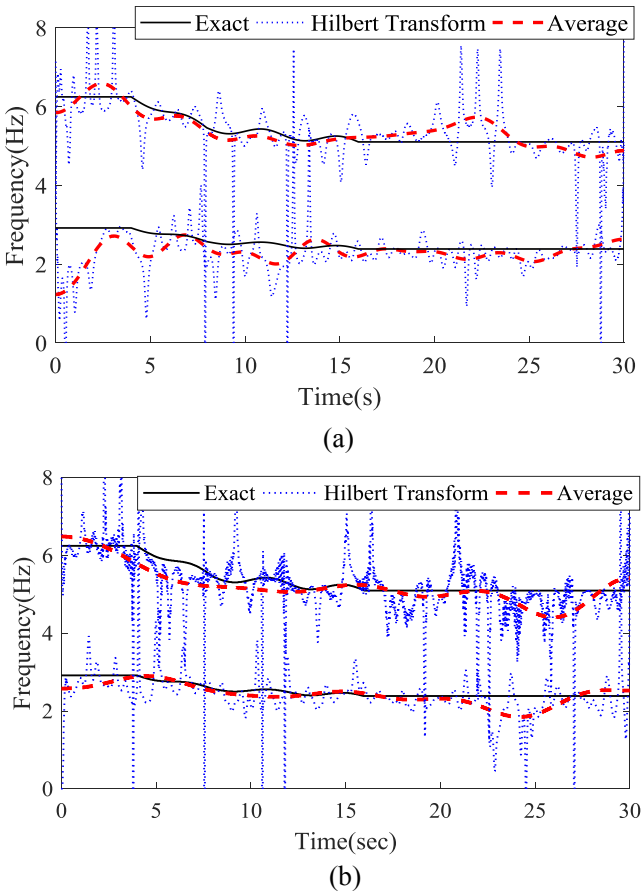

Fig. 13. The identified frequencies of the time-variant structure: (a) Case 1; (b) Case 2.

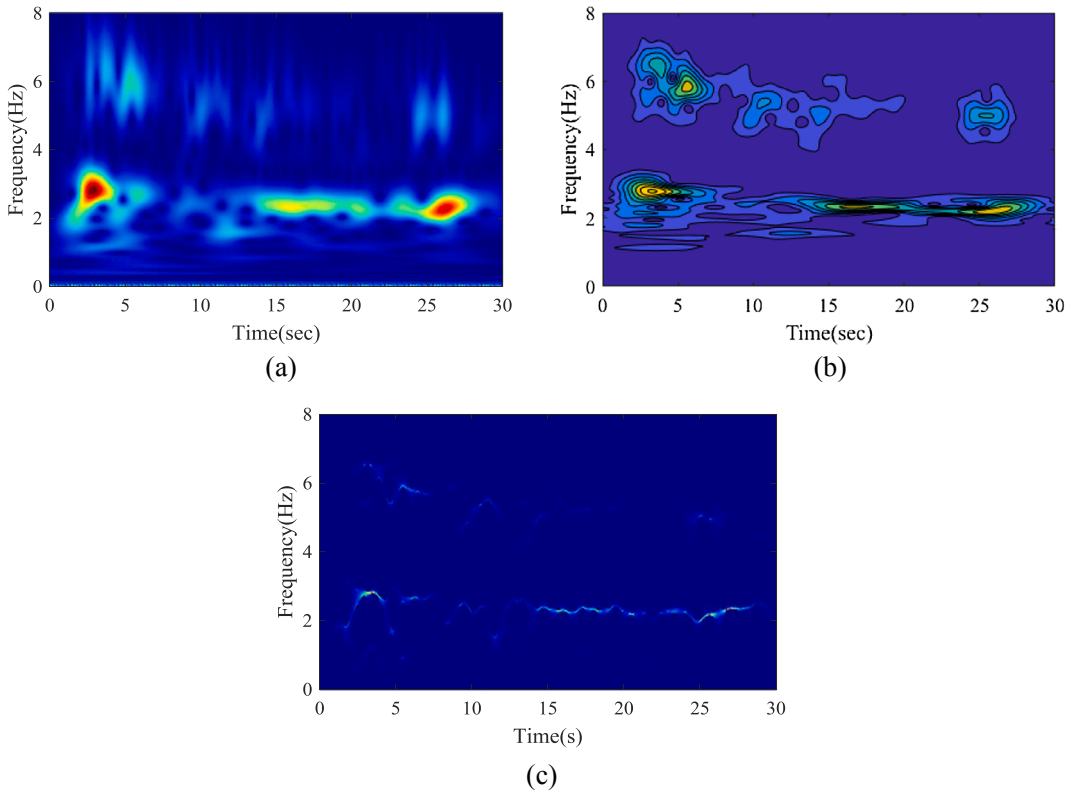

Fig. 12. Time-frequency representation of structural dynamic responses under earthquake excitations: (a) Wavelet Transform; (b) S-Transform; (c) SST;

HT with the exact values. By filtering out the rapidly varying component of the identified instantaneous frequencies using a low-pass filter with a cutoff frequency, the average value of these instantaneous frequencies can reliably denote the natural frequency of the structure under the external excitations.

3.2.2. Effects of measurement noise

To further investigate the performance and reliability of the proposed approach, 5% and 10% noises are added to the structural dynamic responses obtained in Case 1 and Case 2. The same procedure as above is followed to analyze the data. The extracted average frequency components from the two decomposed modes under the effects of the different noise levels are depicted in Fig. 14(a) and (b). It can be observed that the identified instantaneous frequencies are close to the exact values even if under the effects of high-level noise. To further quantify the accuracy of the identified instantaneous frequencies under the effects of measurement noise, an error index *EI* is defined as a root-mean-squared value over the total time duration T of structural dynamic responses,

$$EI = \frac{\sqrt{\int_0^T [IF_a(t) - IF_e(t)]^2 dt}}{\sqrt{\int_0^T [IF_e(t)]^2 dt}} \tag{28}$$

in which $IF_a(t)$ and $IF_e(t)$represent the average and exact instantaneous frequencies, respectively.

Based on Eq. (28), the calculated *EI* values of the identified instantaneous frequencies under the effects of measurement noise are listed in Table 1. In addition, the identified results without the effects of measurement noises are also calculated in Table 1. As can be seen from Table 1, the *EI* values are 9.04% and 5.13%, respectively, under the El Centro earthquake excitation without measurement noise. Similarity, the values are respectively 7.53% and 5.35% under Gaussian white noise excitation. By comparing the calculated *EI* values under various cases, it can be found that the increased noise levels have a slight influence on the identification accuracy.

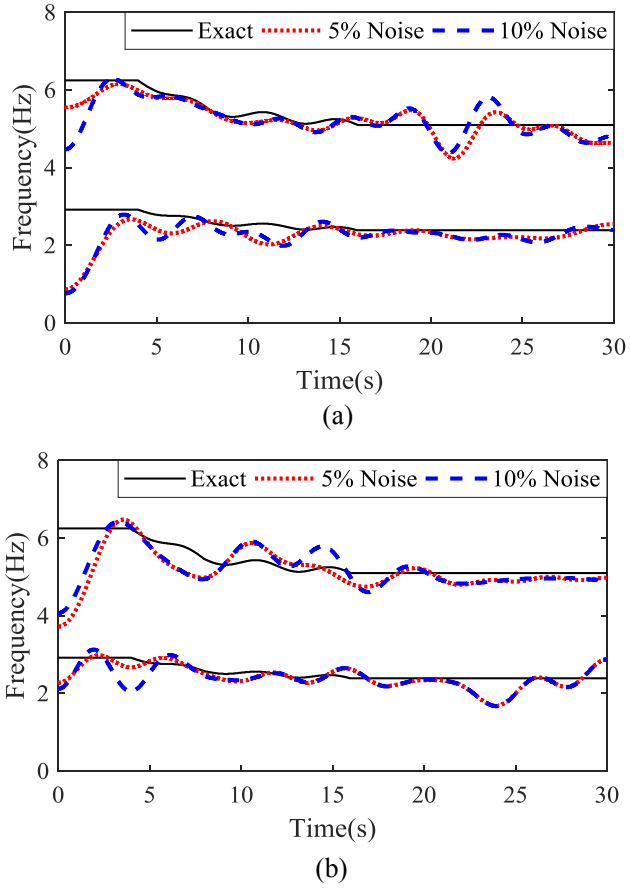

Fig. 14. The identified instantaneous frequencies under different noise levels: (a) under earthquake excitation; (b) under Gaussian white noise excitation.

Table 1
The calculated results of *EI* index.

	Case 1		Case 2	
	Mode 1	Mode 2	Mode 1	Mode 2
Without noise	9.04%	5.13%	7.53%	5.35%
5% noise	9.27%	5.49%	7.71%	6.54%
10% noise	9.45%	6.08%	7.94%	6.83%

It is noticed from Fig. 14(a) and (b) that the identification errors are located at the beginning and/or end of the time series due to the large frequency oscillations. The phenomena is caused by the end effects associated with HT for a finite-length frequency modulated signal, it could not be eliminated completely since the instantaneous frequencies vary with time and the target signal is non-stationary for time-varying systems [12]. Satisfactory results based on the proposed approach are obtained accurately even under significant measurement noise effect.

4. Experimental investigations

4.1. A highway bridge

To further validate the performance of using the improved EWT process for structural time-varying dynamic characteristic identification, experimental studies on an operational highway bridge are conducted. The target bridge consists of three spans, which is shown in Fig. 15. The beams are 17.10 m long in the 1st and 3rd spans, and the central-span beam is 16.96 m long with two half joints at the ends. The half joints shown in Fig. 15(b) have been strengthened by using external vertical steel strengthening rods as well as the horizontal strengthening rods on the two sides of the joint. This half-joint arrangement is different from the typical arrangement as there is no bearing between the suspended and supporting nibs while the joints are post-tensioned by an internal tendon crossing the joint. On the abutments and piers, the girders are tied by cast-in-situ infill panels, which are supported by two 4-column piers. The dynamic responses of the operational bridge system under the traffic loads are recorded by a structural health monitoring (SHM) system installed in 2014. Structural responses, including strain, displacement and acceleration responses, at various locations of the bridge system are measured. The acceleration data of the bridge under the traffic loads are recorded with two tri-axial accelerometers (S_1, S_2) at the mid-span of the bridge. The locations of the acceleration sensors are shown in Fig. 16. A camera is installed to capture the traffic vehicles on the bridge when the SHM system is activated, with a frame rate of 1 Hz. The health monitoring system can be trigged to record the dynamic responses data of the bridge subjected to the traffic when the strain response in any of the strain rings reaches a pre-defined threshold (equals to120 $\mu\varepsilon$). A two minutes window with 60 s pre-triggering and 60 s afterwards is applied to record the dynamic responses of an event with a sampling rate of 130 Hz. Since only two accelerometers are installed at the mid-span of the bridge system to record structural vibration signals, the natural frequencies of the bridge system under the different traffic loading and environmental conditions can be identified, however the mode shape could not be obtained in this case.

Fig. 15. An operational highway bridge: (a) Bird view of the bridge; (b) The reinforced half joints.

4.2. Time-varying instantaneous frequency identification

In this section, operational modal identification of the bridge system under the weak external excitation is conducted, and then the instantaneous frequencies identification of the bridge under heavy traffic loads is further discussed and investigated by using the proposed approach. Based on the images captured by the installed camera, a light weight traffic excitation case is selected for the first case. In this event, the traffic and the measured acceleration response from the accelerometer S_1 are presented in Fig. 17(a) and (b). It can be seen from the measured vibration signal that the maximum response amplitude of the measured acceleration signal is approximately equal to 0.007 g, which can be considered as a relatively small dynamic response measured from the highway bridge. Due to the light weight traffic and the mass of those vehicles is negligible as compared to that of the bridge, the measured acceleration signal is used for the modal identification of the operational bridge system to understand the vibration characteristics of the bridge. However, since the global mode shapes of the structure cannot be obtained by only using the responses at two locations from two accelerometers, a finite element model, as shown in Fig. 18, developed based on the design drawings is employed to approximately represent the bridge. The analytical natural frequencies and the corresponding mode shapes obtained from the finite element model are described in Fig. 19(a)–(d), respectively. By cross checking the frequencies and mode shapes, four main frequencies of the measured vibration signal are identified by performing the fast Fourier Transform

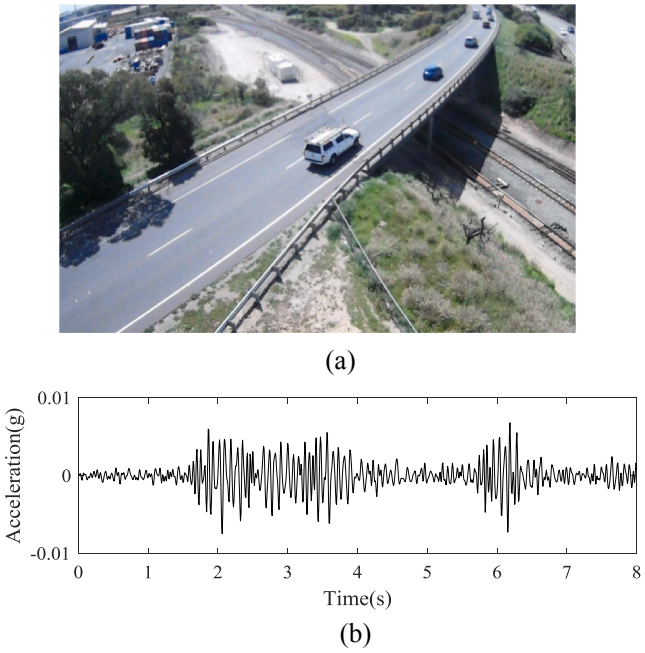

Fig. 17. (a) The light weight traffic excitation; (b) the measured acceleration from sensor S_1.

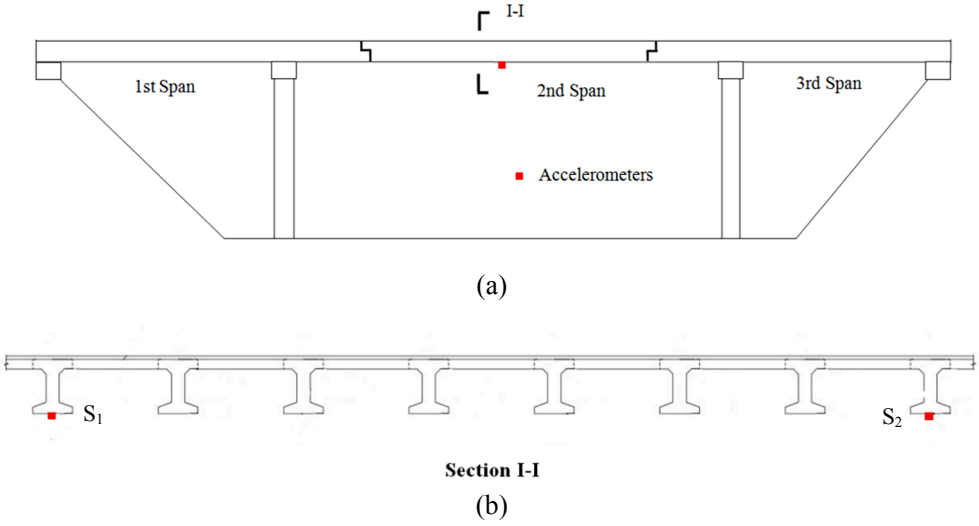

Fig. 16. Locations of the installed accelerometers; (a) Elevation view; (b) Cross section of the mid-span.

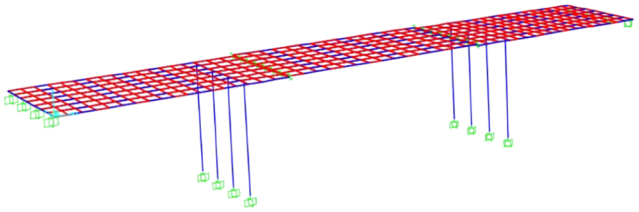

Fig. 18. The bridge model.

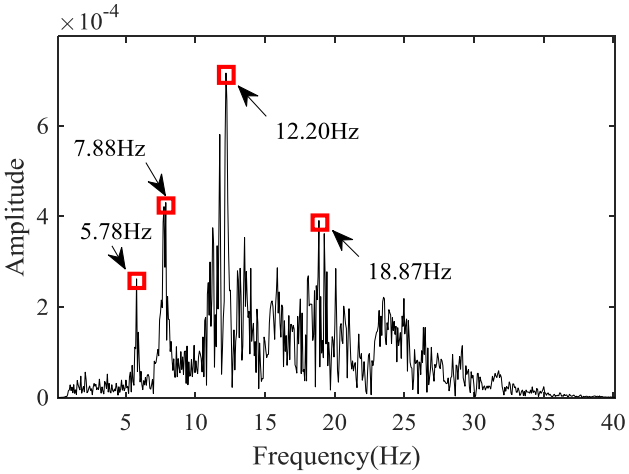

Fig. 20. Fourier spectrum of the measured vibration signal.

as 5.78 Hz, 7.88 Hz, 12.20 Hz and 18.87 Hz, respectively, as shown in Fig. 20. To ensure the reliability of the identified modes, the phase information of each mode extracted from the vibration signals recorded by two accelerometers are compared in Fig. 21(a)–(d), respectively. It can be seen from Fig. 20 that the two vibration signals have similar phase information at the first and the third modes, however, the opposite phase is clearly observed at the second and the fourth modes. Compared with the mode shapes from the finite element model, it can be concluded that the first and third modes correspond to the bending modes of the bridge structure. However, the second and fourth modes are the torsional modes of the bridge. For bridges under traffic loads, higher modes are normally considered to have relatively lower contributions to the responses than the lower modes [29], however, it is observed that the third mode of the bridge at 12.20 Hz has the highest energy in the Fourier Spectrum. The potential reason can be described as: with the roughness and damaged surface on the pavement of the deck, for example, as shown in Fig. 22, the highway bridge is usually forced by the bouncing motion of the moving traffic loads [30–32], which may excite the high frequency components of the bridge.

The natural frequencies of the bridge are verified by performing the finite element analysis. The instantaneous frequencies of the bridge system under the heavy traffic loads are identified by using the proposed approach. The measured acceleration response under two heavy tank trucks is used to identify the time-varying instantaneous frequencies of the structure. The traffic from the selected event and the corresponding vibration signal recorded from the accelerometer S_1 are shown in Fig. 23(a) and (b), respectively. Since the mass ratio between two heavy tank trucks and the bridge is more significant than the first case, the bridge is considered as a time-varying system when the vehicles are crossing the bridge. The maximum recorded acceleration signal on the bridge is equal to 0.048 g, indicating a significant vibration. In order to identify the varying modes of the acceleration signal, the time-frequency analysis based on SET is first performed to determine the frequency boundaries of the modes. The time-frequency analysis results from SET are shown in Fig. 24(a) and (b), and it is clearly observed that the filtering boundaries of EWT can be determined. To extract two bending modes from the non-stationary acceleration signal, the filtering boundaries of 4.8 Hz, 6.8 Hz, 9.5 Hz and 14.2 Hz are selected for EWT. It can be noted from Fig. 24(a) that the time resolution of the first two time-variant modes is low, and the main reason is the time series used in this study is too short, which would cause a low time resolution due to the requirement of frequency resolution. Once the two bending modes are accurately extracted from the non-stationary acceleration signal via EWT, the instantaneous frequencies of two modes can be identified and shown in Fig. 25(a) and (b), respectively. It can be observed from Fig. 25 that these two identified instantaneous frequencies by using HT method have a slow fluctuation trend when the two heavy trucks are crossing the bridge. By filtering out the rapidly varying component of the identified instantaneous frequencies using a low-pass filter with a cutoff frequency of 0.1 Hz, the average instantaneous frequencies are extracted and shown in Fig. 25. As observed from Fig. 25(a), the IF of the first bending mode is gradually changing from 5.96 Hz to 4.88 Hz, and coming back to 5.64 Hz at the end of the event. This demonstrates that the bridge under heavy trucks in this case is time-varying, due to the significant mass ratio between the two heavy trucks and the bridge [31,32], as well as the varying excitation locations. Due to the heavy mass of the vehicle, the total mass of the bridge-vehicle system increases and therefore the identified natural frequency decreases. As observed from

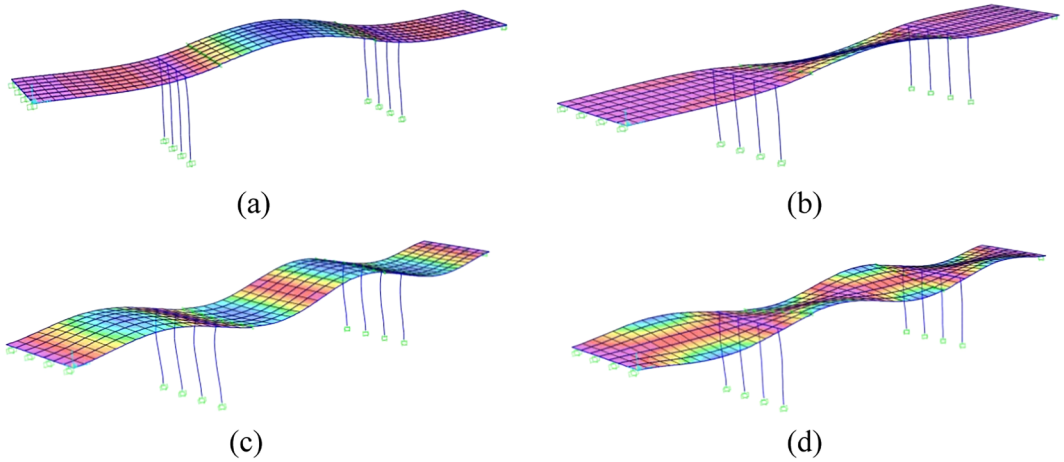

Fig. 19. Modal information extracted from the FE model: (a) Mode 1 (f_1 = 5.82 Hz); (b) Mode 2 (f_2 = 7.85 Hz); (c) Mode 3 (f_3 = 12.85 Hz); (d) Mode 4 (f_4 = 16.77 Hz).

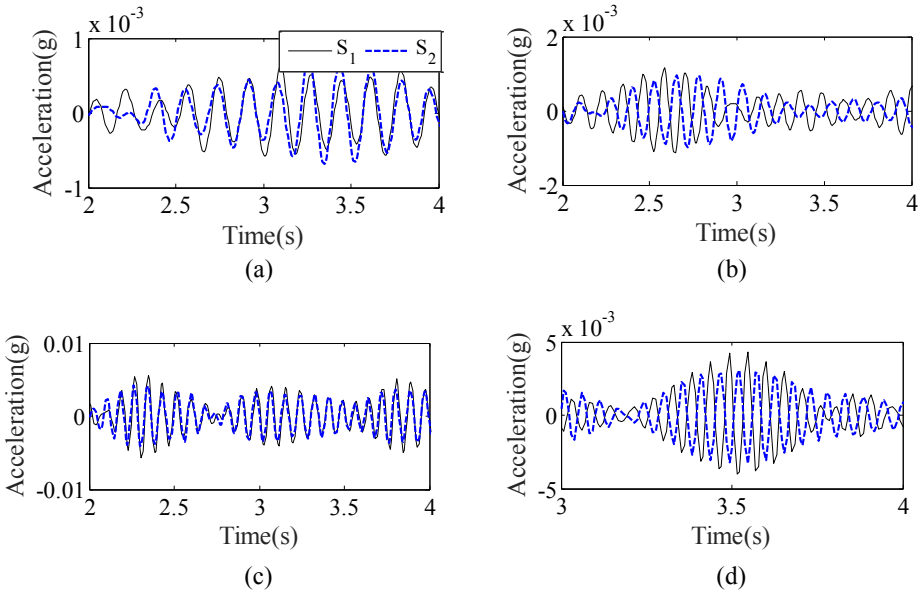

Fig. 21. The phase information of each mode between two measured acceleration signals: (a) Mode 1; (b) Mode 2; (c) Mode 3; (d) Mode 4.

Fig. 22. The damaged surface of the bridge deck.

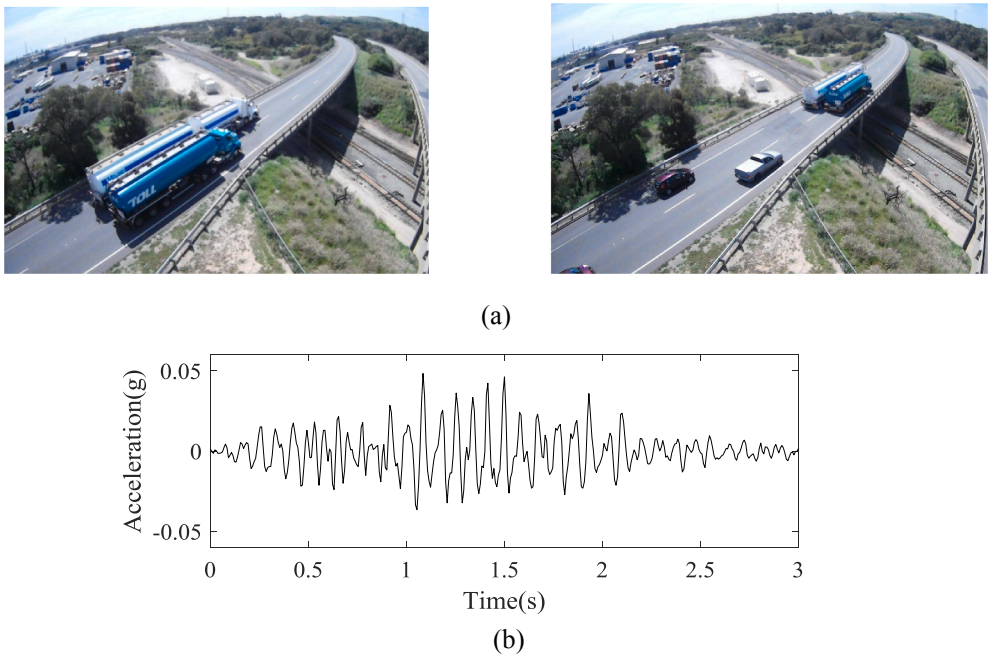

Fig. 23. (a) The traffic loads on the bridge; (b) the corresponding measured acceleration from S1.

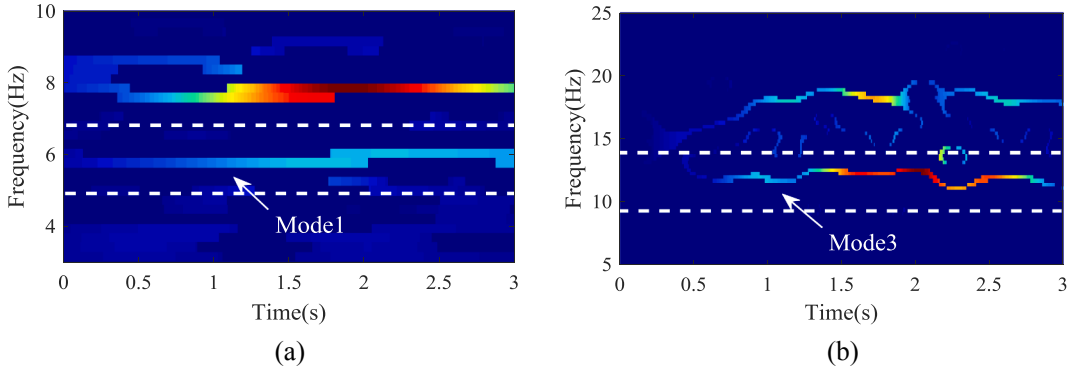

Fig. 24. The two identified bending modes based on the results of SET: (a) Mode1; (b) Mode3.

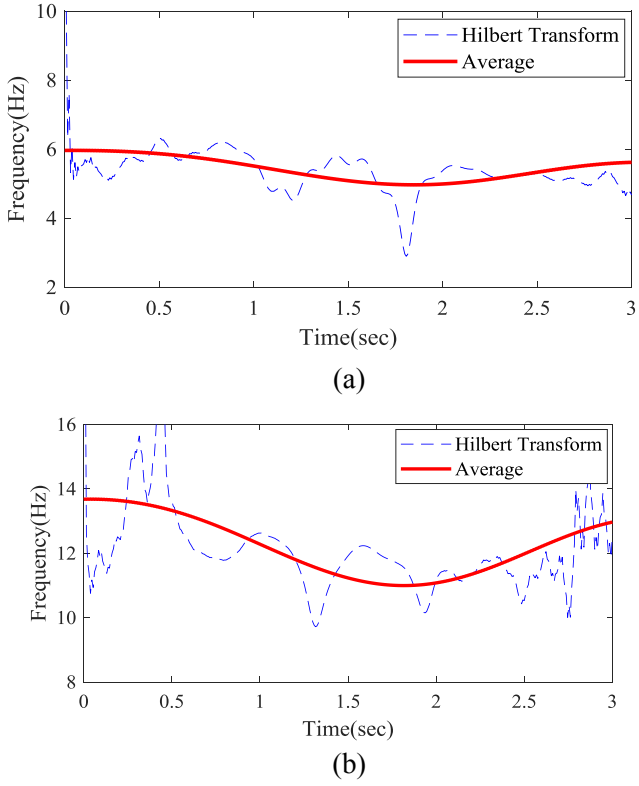

Fig. 25. The identified instantaneous frequencies of two bending modes via the proposed approach: (a) The first bending mode; (b) The second bending mode.

Fig. 25(b), the IF of the second bending mode of the measured acceleration signal shows a similar variation pattern as the first bending mode. The maximum change rate of the IF is approximately equal to 19.5%, which indicates that the heavy traffic loads have a significant effect on the modal parameters of the highway bridge. Generally, it can be concluded that the proposed approach can well separate the two main time-varying modes from a non-stationary vibration signal, as well as track the IF of a time-varying bridge-vehicle system.

5. Conclusions

This paper proposes an enhanced EWT approach based on SET for the time varying system identification. The time-frequency analysis of a vibration signal is performed by using SET to determine the filtering boundaries of EWT analysis instead of using Fourier Spectrum. An enhanced EWT method is developed to separate the vibration signal into several IMFs based on the predefined filtering boundaries. When IMFs of a vibration signal are obtained, HT can be conducted to identify and extract IF of each mode. The slowly varying part of the identified instantaneous frequencies by HT is approximately equal to the instantaneous frequencies of a time-varying system under the external excitations. Based on the results of both numerical simulations and experimental validations, the corresponding conclusions can be concluded as following:

(1) The improved EWT approach with SET can be used to accurately decompose a non-stationary signal into several modes based on the predefined filtering boundaries from SET;
(2) The proposed approach is effective and accurate for time-varying system identification to obtain the instantaneous frequencies of structures, even under the significant noise effect.

Acknowledgements

The work described in this paper was financially supported by China Scholarship Council Postgraduate Scholarship No. 201606690031, and Australia Research Council Linkage project LP160100528. The support and permission granted by Main Roads Western Australia (MRWA) to use the data and publish the information in this study are thankfully acknowledged. Conclusions drawn from the data provided by MRWA are those of the authors based on the conducted analyses/evaluations and do not necessarily represent the views of MRWA.

Appendix A. Supplementary material

Supplementary data to this article can be found online at https://doi.org/10.1016/j.engstruct.2019.109313.

References:

[1] Wang ZC, Ren WX, Chen GD. Time-varying linear and nonlinear structural identification with analytical mode decomposition and Hilbert transform. J Struct Eng ASCE 2013;139(12):06013001.
[2] Bao CX, Hao H, Li ZX, Zhu XQ. Time-varying system identification using a newly improved HHT algorithm. Comput Struct 2009;87(23–24):1611–23.
[3] Huang Q, Xu YL, Liu HJ. An efficient algorithm for simultaneous identification of time-varying structural parameters and unknown excitations of a building structure. Eng Struct 2015;98:29–37.
[4] Tang HS, Xue ST, Chen R, Sato T. Online weighted LS-SVM for hysteretic structural system identification. Eng Struct 2006;28(12):1728–35.
[5] Lin JW, Betti R, Smyth AW, Longman RW. On-line identification of nonlinear hysteretic structural system using a variable trace approach. Earthq Eng Struct Dyn 2001;30:1279–303.
[6] Yang JN, Huang HW. Sequential non-linear least-squares estimation for damage identification of structures with unknown inputs and unknown outputs. Int J Non Linear Mech 2007;42(5):789–801.
[7] Wang C, Ren WX, Wang ZC, Zhu HP. Instantaneous frequency identification of time-varying structures by continuous wavelet transform. Eng Struct 2013;52:17–25.
[8] Wang ZC, Ren WX, Chen GD. Time-frequency analysis and applications in time-varying nonlinear structural systems: A state-of-the-art review. Adv Struct Eng 2018;21(10):1562–84.
[9] Wang ZC, Xin Yu, Xing JF, Ren WX. Hilbert low-pass filter of non-stationary time sequence using analytical mode decomposition. J Vib Control

2017;23(15):2444–69.
[10] Smyth AW, Masri SF, Chaassiakos AG, Caughey TK. Development of adaptive modeling techniques for non-linear hysteretic system. Int J Non Linear Mech 2002;37(8):1435–51.
[11] Noel JP, Kerschen G. Nonlinear system identification in structural dynamics: 10 more years of progress. Mech Syst Sig Process 2017;83(15):2–35.
[12] Wang ZC, Ren WX, Chen GD. Analytical mode decomposition of time series with decaying amplitudes and overlapping instantaneous frequencies. Smart Mater Struct 2013;22(14):095003.
[13] Dziedziech K, Staszewski WJ. Wavelet-based modal analysis for time-variant systems. Mech Syst Sig Process 2015;50–51:323–37.
[14] Klepka A, Uhl T. Identification of modal parameters of non-stationary systems with use of wavelet based on adaptive filtering. Mech Syst Sig Process 2014;47(1–2):921–34.
[15] Ulker-Kaustell M, Karoumi R. Application of the continuous wavelet transform on the free vibrations of a steel-concrete composite railway bridge. Eng Struct 2011;33(3):911–9.
[16] Shi ZY, Law SS. Identification of linear time-varying dynamical systems using Hilbert transform and empirical mode decomposition method. J Appl Mech 2007;74(2):223–30.
[17] Wang ZC, Chen GD. Recursive Hilbert-Huang transform method for time-varying property identification of linear shear-type buildings under base excitations. J Eng Mech ASCE 2012;138(6):631–9.
[18] Hou ZK, Hera A, Shinde A. Wavelet-based structural health monitoring of earthquake excited structures. Comput-Aided Civ Infrastruct Eng 2006;21:268–79.
[19] Daubechies I, Lu JF, Wu HT. Synchrosqueezed wavelet transforms: an empirical mode decomposition-like tool. Appl Comput Harmon Anal 2011;30(2):243–61.
[20] Liu JL, Wang ZC, Ren WX, Li XX. Structural time-varying damage detection using Synchrosqueezing wavelet transform. Smart Struct Syst 2015;15(1):119–33.
[21] Wang S, Chen X, Cai G, Chen B, Li X, He Z. Matching demodulation transform and synchrosqueezing in time-frequency analysis. IEEE Transac Signal Process 2014;62(1):69–84.
[22] Yu G, Yu MJ, Xu CY. Synchroextracting transform. IEEE Trans Ind Electron 2017;64(10):8042–54.
[23] Gilles J. Empirical wavelet transform. IEEE Transac Signal Process 2013;61(16):3999–4010.
[24] Xin Y, Hao H, Li J. Operational modal identification of structures based on improved empirical wavelet transform. Struct Control Health Monitor 2019;26:e2323.
[25] Amezquita-Sanchez JP, Park HS, Adeli H. A novel methodology for modal parameters identification of large smart structures using MUSIC, empirical wavelet transform, and Hilbert transform. Eng Struct 2017;147:148–59.
[26] Wang SB, Chen XF, Tong CW, Zhao ZB. Matching synchrosqueezing wavelet transform and application to aeroengine vibration monitoring. IEEE Trans Ind Electron 2017;66(2):360–72.
[27] Oberlin T., Meignen S., Perrier Valérie. The Fourier-based Synchrosqueezing Transform. 2013. Hal-00916088.
[28] Ni PH, Li J, Hao H, Xia Y, Wang XY, Lee JM, et al. Time-varying system identification using variational mode decomposition. Struct Control Health Monitor 2018;25:e2175.
[29] Kim J, Lynch JP. Experimental analysis of vehicle-bridge interaction using a wireless monitoring system and a two-stage system identification technique. Mech Syst Sig Process 2012;28:3–19.
[30] Cantieni R. Investigation of vehicle-bridge interaction for highway bridges. Heavy vehicles and roads: technology, safety and policy London. Thomas Telford; 1992.
[31] Xiao F, Chen GS, Hulsey JL, Zatar W. Characterization of non-stationary properties of vehicle-bridge response for structural health monitoring. Adv Mech Eng 2017;9(5):1–6.
[32] Cantero D, Hester D, Brownjohn J. Evolution of bridge frequencies and modes of vibration during truck passage. Eng Struct 2017;152:452–64.